Research Square

Preprints are preliminary reports that have not undergone peer review.
They should not be considered conclusive, used to inform clinical practice,
or referenced by the media as validated information.

Riparian corridors across a persistent arid belt challenge the widespread greening of the Holocene Sahara

Katie Manning

katie.m.manning@kcl.ac.uk

King's College London https://orcid.org/0000-0002-8512-156X

Paul Breeze

King's College London https://orcid.org/0000-0003-2575-8021

Nick Drake

Kings College London

Adrian Timpson

University College London https://orcid.org/0000-0003-0292-8729

Article

Keywords: African Humid Period, Green Sahara, Biogeography, Palaeohydrology, Climate Change, Palaeoclimate

Posted Date: November 26th, 2026

DOI: https://doi.org/10.21203/rs.3.rs-11610542/v1

License: This work is licensed under a Creative Commons Attribution 4.0 International License.
Read Full License

Additional Declarations: There is **NO** Competing Interest. No competing interests

Riparian corridors across a persistent arid belt challenge the widespread greening of the Holocene Sahara

Katie M. Manning[1], Paul S. Breeze[1], Nick A. Drake[1], Adrian Timpson[2]

[1] Department of Geography, King's College London, London, WC2B 4BG, United Kingdom
[2] Research department of Genetics, Evolution and Environment, University College London, London, WC1E 6BT, United Kingdom
Correspondence to: Katie M. Manning (katie.m.manning@kcl.ac.uk)

Abstract

The extent and continuity of humid conditions across the Sahara during the Holocene African Humid Period remain highly debated, with palaeoenvironmental proxy records and climate models providing contrasting interpretations of the timing, magnitude, and spatial extent of hydroclimatic change. Resolving these uncertainties is critical for understanding how North African environments have shaped, and may continue to influence, the distribution and dispersal of human and animal populations, while also improving climate projections by better constraining the land–atmosphere feedback associated with Saharan greening. Here, we present a novel, spatially explicit reconstruction of Holocene water availability and biogeography by integrating palaeohydrological mapping, >1100 radiocarbon dates associated with hydrological activity, and bioclimatic constraints derived from >135,000 faunal remains. Our results estimate the maximum expansion of two weather systems (the West African Monsoon (WAM) from the south, and the Mediterranean winter precipitation (MWP), driven by the Westerlies, from the north) occurred at 7790 BP but did not meet, leaving a persistent arid zone. However, we also find that this arid zone was traversed by riparian corridors, providing potential dispersal routes through the Sahara for highly mobile species such as humans. Rather than a continuous Sahelian ecosystem extending across the Sahara, our reconstruction reveals a heterogeneous Sahara. These results challenge interpretations of a uniformly "Green Sahara" and show how climate change affects hydrological connectivity and can create dispersal pathways across otherwise inhospitable landscapes.

Keywords

African Humid Period; Green Sahara; Biogeography; Palaeohydrology; Climate Change; Palaeoclimate

1. Introduction

The most recent African Humid Period (AHP), otherwise known as the 'Green Sahara', occurred between c. 14,000 and 5000 yrs BP, and was characterised by increased effective precipitation [1], more vegetation [2], higher lake levels [3] and a significant increase in human occupation [4]. The onset and termination of the AHP is widely recognised to be the result of changes to northern hemisphere insolation resulting from slow shifts in the Earth's orbit which led to an expansion and contraction of the West African Monsoon (WAM) [5-7]. However, there remains considerable uncertainty about how the Green Sahara evolved temporally and regionally, and specifically how 'green' it really was. Gaining clarity on these issues is key to understanding how gradual climate forcing can result in rapid and widespread climate responses, the impact this can have on human and other animal populations both in the past and future, and to what extent the Sahara may have provided barriers or corridors to human mobility during the Holocene. Resolving the sensitivity of Saharan greening to climate forcing will also improve our understanding of telecoupled climate impacts, including how climate-driven changes in one region can influence environmental conditions and human populations in distant, interconnected regions. Recent modelling studies, for example, have demonstrated that Saharan greening influenced atmospheric circulation far beyond North Africa, altering Northern Hemisphere circulation patterns, including the North Atlantic and North Pacific jet streams[8], as well as tropical Atlantic–Pacific climate interactions and El Niño–Southern Oscillation (ENSO) variability [9, 10]. These findings highlight the

importance of accurately reconstructing the spatial extent and character of Saharan greening for understanding regional climate feedbacks and their wider global consequences.

Early evidence for large-scale environmental change in the Sahara emerged from palaeohydrological and geomorphological studies demonstrating that regions now characterised by extreme aridity contained extensive lake systems during the early and middle Holocene. In particular, the work of Street and Grove [5] and Street-Perrott and colleagues [11] provided the first continental-scale syntheses of African lake-level changes, demonstrating a major increase in effective moisture across North Africa during the Holocene. These studies transformed our understanding of the Sahara from a climatically stable desert environment to a dynamic system capable of undergoing substantial hydrological reorganisation in response to orbital forcing. In parallel, pioneering climate modelling studies demonstrated that the magnitude and abruptness of Saharan environmental change could not be explained by orbital forcing alone. Claussen and colleagues showed that vegetation–atmosphere feedbacks, particularly interactions between vegetation cover, surface albedo and monsoon circulation, could amplify the climate response and contribute to the rapid expansion and contraction of Saharan vegetation [12, 13]. Subsequent palaeoenvironmental syntheses expanded this framework, using pollen, palaeohydrological and archaeological evidence to reconstruct the extent of humid environments and the associated expansion of vegetation, aquatic systems, and human occupation [2-4, 14, 15].

Marine sediment records further developed the concept of the Green Sahara by providing continuous records of Saharan environmental change. Multiple marine core sediment studies from the Mediterranean basin [16], northwest African coast [17, 18] and Gulf of Aden [1, 19] have been used to infer a humid climate as far north as 31°N. However marine records derive their source particulates from large but poorly defined regions of the Sahara, which are subject to complex wind patterns before their final deposition. As a result, their interpretation offers widely conflicting views on how far north rainfall penetrated during the AHP. For example, analysis of dust accumulation rates from the Red Sea, suggest that humid conditions did not extend into the northeastern Sahara north of ~22°N [20]. In contrast analysis of δD_{wax} records from marine cores along the northwest African coast indicate that WAM rainfall penetrated as far north as the Atlas Mountains and that the entire Sahara was green, though the correlation between dust flux and δD_{wax} derived precipitation rates is notably weaker in the most northern marine core sediment (e.g. core site GC27) suggesting that the δD_{wax} record might be biased by the Atlas Mountains where precipitation originates from the Westerlies weather systems penetrating south from the Mediterranean [21].

Marine core sediments from the northwest African coast [1] have also been used to date the onset and termination of humid conditions, indicating a rapid hydroclimatic shift between 12,500 -11,500 and 5500 years BP. While these records provide important archives of regional-scale North African hydroclimatic variability, their spatial interpretation remains challenging because dust and biomarker signals integrate material transported from multiple source regions across the Sahara (e.g. [17, 22]. As a result, the precise location and extent of the terrestrial environments represented by these marine records remains debated. The Bodélé Depression located at 17°N, for example, is believed to emit 0.7 million tons of dust per day [23], making it the world's greatest single dust source. It also shows a rapid drying event at 5000 BP [24], which aligns well with the marine record from

ODP core 658C [17, 25]. In contrast, pollen and sedimentological records from Lake Yoa in northern Chad suggest that the termination of humid conditions may have been gradual and progressive [26, 27] although the contribution of groundwater to the lake complicates the situation. Though Lake Yoa is the remnant of a much larger lake, it is still in existence today and is almost exclusively fed by permanent groundwater outflow from a regional aquifer. Similarly, some of the northern palaeolakes e.g. Hassi el Mejnah and Sebkha Mellala display larger water volumes during the AHP [28, 29], yet they probably reflect a component of groundwater discharge which is recharged at the M'zab mountains, rather than direct precipitation [28]. Importantly, however, groundwater was not the only mechanism by which water could be transferred from wetter highland regions into the arid Saharan interior. Sebkha Mellala, for example, continues to receive episodic surface runoff from the Atlas Mountains to the north, illustrating how precipitation falling outside the desert interior can be routed considerable distances through drainage networks. During wetter periods, activation of such catchments and river systems could therefore have sustained lakes and riparian environments far beyond the areas receiving the precipitation itself. This distinction between local precipitation and remotely sourced surface-water inputs is important when reconstructing the spatial extent of humid conditions across the Sahara.

Unlike marine cores, terrestrial proxy records, such as sedimentological and palaeohydrological data, provide important information at specific and well-defined locations. Pollen records demonstrate that savanna vegetation and tropical plants migrated as far as 24°N after which it is argued that the Sahara was composed of a steppe biome [2, 14]. Palaeohydrological evidence meanwhile suggests palaeolakes up to 28°N [3]. These data have also been used to assess regional heterogeneity in humid tropical conditions. For example, some sub-Saharan aquatic species do not exhibit trans-Saharan spatial distributions, which suggests variation in the extent of surface water within the Sahara [30]. Patches of relatively arid terrain within a more humid environment, for example, have been hypothesized in parts of the Central Sahara based on pollen core records from Holocene lakes in the region [2]. A combination of pollen records and stable hydrogen isotope compositions (δD) in leaf wax from lake Tislit in the high Atlas mountains have also been used to infer the source of precipitation [31], which the authors suggest is indicative of the Northern Hemisphere's winter storm track and the westerly jet stream.

These uncertainties have led to an increasing focus on the interaction between the northward expansion of the West African Monsoon (WAM) and the potential southward influence of Mediterranean Winter Precipitation (MWP), which is driven by the Westerlies. During periods of maximum boreal summer insolation and minimum boreal winter insolation, such as the Early Holocene, the equator-to-pole temperature gradient weakened during winter, driving a southern shift of the Hadley cell, Westerlies and Mediterranean storm track and bringing increased winter precipitation to northern Africa [32]. Using a range of proxy datasets and modelling experiments, Wagner et al. [33] support this mechanism, proposing that North Atlantic low-pressure systems may have periodically extended from the Mediterranean into northern Sahara. More recent data suggest that the Westerlies may have contributed to greening of the desert as far south as the Tibesti mountains [34]. Whilst these studies help to reconcile some disparities between Holocene climate model simulations and proxy datasets, there remains the fundamental question of whether these two weather systems overlapped, if so for how long, or if an arid belt persisted between them [31].

Resolving this question has increasingly relied on the integration of proxy records and generative climate modelling. However, there is considerable disagreement both within and between these two approaches such that General Circulation Models (GCMs) fail to reproduce the precipitation increase inferred from palaeoclimate proxy data [1, 35, 36]. Whilst summer insolation increase is known to enhance monsoon circulation and precipitation, a number of additional feedback processes, including dynamic dust [37] vegetation [38], and lakes and wetlands [39], have been hypothesised to augment GCMs locally, and therefore explain the magnitude of change during the early to mid-Holocene [40]. Despite the addition of these feedback processes, however, considerable disagreement remains in model outputs, partly as a result of limited validation data, particularly in the northernmost latitudes of the Sahara.

One way to overcome the discrepancies between paleoclimate proxy datasets is to employ palaeoclimate models, although until recently these have consistently struggled to predict a green Sahara during the most recent AHP, when proxy data are most abundant [35, 41-43]. Considerable effort has therefore been expended to incorporate new land surface processes into models to provide a more realistic simulation of climate change in semi-arid and arid environments. These studies have found that incorporating lakes or vegetation [38, 39, 44] makes the Sahara greener than in previous models, whilst dust and vegetation allows Saharan greening in some models [37, 45], but not in others [46]. Pausata and colleagues [37], for example, indicate a maximum extent of monsoon rains to 31°N with prescribed vegetation and dynamic dust, compared to 26°N with just prescribed vegetation and only 16°N with orbital forcing alone. Hopcroft and Valdes [46], meanwhile, included a fully interactive dust cycle in the HadGEM2-ES model, demonstrating only a small rainfall feedback with dust.

A recent combined analysis of sedimentary data, climate modelling and water balance modelling [34] suggests that strong orographic uplift of moist air masses in the south-central Sahara may have been brought in by north-easterly winds from the Mediterranean, not by the West African monsoon from the south. Whilst the West African monsoon appears to have reached the Tibesti mountain region during the early Holocene, Hoelzmann and colleagues [34] argue that it was too weak to be uplifted to the higher crater lakes, located around 21°N and 16.5°E. However, the underpinning climate model in this analysis fails to capture observed wetness in more northern regions of the Sahara e.g. Takakori in the Tadrart Acacus at 24.5°N [47], where wet environmental conditions are evidenced by pollen, fish remains and geomorphological features, suggesting a source of error in the simulated moisture fluxes from Jungandreas et al. [48, 49]. Cheddadi et al. [31] present a set of idealised scenarios which incorporate a hypothesised extension of the Westerlies to at least 24° N and potentially 18° N based on lake core evidence from Lake Tislit. They achieve a ‘green’ Sahara throughout the Holocene, which they argue shows that the Westerlies and WAM ‘...must have met and possibly overlapped’. Therefore, whilst new proxy data provides valuable insight into the southward expansion of the North Atlantic climate system and the idealised model parameters help to reconcile the disparity between Holocene climate model simulations and the extant proxy datasets, the questions remain regarding if and where these two weather systems overlap.

Saharan hydroclimatic variability also has implications for longer-term hominin dispersal within and out of Africa. Humid phases are thought to have periodically increased the permeability of the Sahara, with

palaeolakes and drainage networks potentially providing dispersal corridors beyond the Nile Valley [30, 50, 51]. Recent evidence from northern Africa further highlights the importance of heterogeneous, mosaic environments, where localised wetlands and other resource-rich habitats occurred alongside seasonally arid landscapes and may have facilitated hominin occupation and dispersal [52, 53]. Establishing whether such movement required widespread ecosystem greening or could instead have occurred along spatially restricted hydrological corridors, is therefore important for understanding the role of the Sahara in past hominin dispersal. Understanding the sensitivity of Saharan hydrological connectivity to climatic change also has contemporary relevance, as future shifts in rainfall and water availability may reshape the distribution of habitable landscapes, livelihoods and patterns of human mobility across the region.

This paper addresses the core question of how far north the WAM extended, and how far south the Westerlies extended, and their impact on Holocene greening. We use updated trans-Saharan palaeohydrological data alongside a novel bioclimatic indicator, using faunal records from archaeological sites to produce a comparative assessment of water availability through time and space. Faunal remains provide valuable biogeographic information to help understand changing patterns of vicariance, climate and habitat, that when combined with the palaeohydrological data creates a more detailed and robust understanding of the past Saharan hydroclimate.

2. Materials

Our analysis utilised three core datasets: a palaeohydrological map derived from remotely sensed and GIS (Geographic Information System) analyses, radiocarbon dated samples associated with hydrological activity e.g. dateable materials such as freshwater molluscs, marsh deposits, marl, organic sediments and calcareous tufa, and archaeological faunal records with associated radiocarbon dates (Fig. 1 and Fig. 2). These datasets were compiled as part of the Leverhulme-funded Green Sahara project, which developed a comprehensive database of published Holocene archaeological and palaeoenvironmental records across North Africa, including site occupation data, radiocarbon dates, palaeohydrological features, pollen records, faunal assemblages and rock art. Additional primary data, including new isotopic analyses, were also incorporated. While occupation and faunal records were compiled from a wide range of published sources, a substantial component of the palaeohydrological chronology was derived from the synthesis of Lézine et al. [3]. This dataset was quality-controlled to remove duplicate entries and incorrectly attributed dates (e.g. archaeological dates misclassified as hydrological samples) and was expanded through the incorporation of more recently published records, increasing the palaeohydrological dataset from 1300 dates [3] to 2141 dates.

For analysis we restricted our data in three ways: a) we included only sites north of 13 degrees latitude, to capture where endogenous moisture transport could have altered the desert conditions; b) we excluded all samples from the Nile Valley to avoid conflating permanent hydrological activity along the river with monsoon-fed hydrological re-activation; c) we only used samples within our study period of 14ka to 2ka. We therefore used a total of 2005 sites as follows: 1059 sites containing archaeological data; a further 269 sites containing archaeological and faunal data comprising 147,443 total NISP from 1039 taxa records; 622 sites containing hydrological data; and a further 55 sites contained mixed information (Fig 2). Radiocarbon dating from a subset

of these sites permitted us to date 694 archaeological phases from 537 sites, of which 332 phases from 279 sites also contained faunal data; and dated evidence of water from 489 hydrological sites.

3. Methods

3.1 Palaeohydrological feature mapping

Palaeohydrological features were mapped using remote sensing and GIS techniques, applying methodology developed by Breeze et al. [54] to identify relict drainage systems, lakes and wetlands; and methodology from Drake et al. [30] to map the fluvial fans across more than 9 million km^2 of northern Africa [52]. Flow accumulation data were calculated from HydroSHEDS 3AS data [55] to map major surface palaeodrainage at ~90 m resolution, with river networks being classified by thresholding, with contributing upstream flow accumulation areas in excess of 1000 km2. Associated river catchments were calculated using HydroBASINS [56].

3.2 Palaeohydrological catchment activation reconstructions

The identified palaeohydrological features represent aggregated signatures from multiple greening events which created and re-activated local hydrological systems during the course of the Quaternary. Thus, to identify which areas were likely to have been activated during the most recent AHP, we generate catchment activation reconstructions that use HydroBASINS (Lehner and Grill, 2013), which delineate nested watersheds based on Pfaf-stetter ordering. We then specify a catchment as activated if it contains one or more hydrologically associated C^{14} dates within a selected time slice. To systematically choose the best catchment resolution level (varying from HydroBASINS level 1 which places our entire study area in a single catchment, to level 12 which provides 108,240 catchments) we applied a cross validation approach that randomly assigned our hydrologically associated C^{14} dataset into two equally sized partitions, counted the total number of catchments containing C^{14} dates from both partitions (matches), and the total number of catchments containing dates from one partition but not the other (mismatches). We then deducted the total mismatches from the total matches to find which level provides the greatest similarity between the two subsets, which occurs at level 4. At lower levels there are fewer mismatches but also fewer matches; at higher levels there are more matches, but the number of mismatches is even greater (Table S3). To systematically choose the best time bin width we applied a similar cross validation approach that separates level 4 catchments into time bins, and counted the total number of time bin catchments containing C^{14} dates from both partitions (matches). We repeated this for 100 different bin widths from 100 years to 2000 years, and established that the peak match occurred at 500 years (Fig. S2). This allowed us to map activated catchments in 500 year time intervals at level 4, including overlays in wider time intervals, providing a spatiotemporal wetness proxy for the entire Holocene (Fig. 2 and Fig 6).

3.3 Faunal remains as a bioclimatic indicator

Whilst palaeohydrological reconstructions can provide information about the spatial and temporal extent of hydrological reactivation, they provide a weaker proxy for local precipitation and ecological conditions. Both large exogenous river systems, such as the Niger and Nile and large lakes, such as Lake Chad, are well known to traverse desert environments, originating outside the desert and creating riparian environments through what is otherwise an arid environment. These environments do not support large populations of savanna species but create corridors that allow water-dependent species to reach deep into the desert. Therefore, to investigate the broader regional ecological conditions across the whole Sahara, we use faunal remains from archaeological sites. These provide direct archaeological evidence of local animal populations at a given point in time and space and can be used to infer a regional wetness index that can be compared directly with the palaeohydrological data. Because the composition and relative abundance of animal taxa are shaped by environmental conditions, most notably vegetation and surface water availability, faunal assemblages can be used as bioclimatic indicators. We developed a novel Water Dependency Index (WDI) based on two complementary criteria: physiological dependence on drinking water, measured by the maximum number of days a species can survive without drinking, and ecological dependence on permanent water bodies as part of their habitat. As such, the WDI provides a means of reconstructing local ecological conditions along a gradient of water availability and habitat conditions. The relative representation of taxa across WDI1–WDI5 distinguishes faunal communities dominated by arid-adapted species (WDI4-5) from those increasingly reliant on regular surface water (WDI 2-3) and, the most water dependent, requiring permanent aquatic or riparian habitats (WDI 1). The composition of these categories therefore provides an integrated indicator of both local surface-water availability and the associated habitats capable of supporting water-dependent fauna. Whilst 628 different animal taxa were identified, only 236 of the taxa have distinct ecological signatures (e.g. they are not broad-spectrum species and have specific water requirements). All domestic taxa were also excluded from this analysis. Table 1 shows the criteria for each WDI category, and the taxa included in each category.

WDI	Physiological dependence on water	Dependence on permanent water as habitat	Hydro-ecological interpretation	Species included
1 (n=172)	Requires permanent water.	Very high – aquatic or semi-aquatic habitat required	Permanent aquatic environments – rivers, lakes and other persistent surface-water bodies	172 entries encompassing freshwater fish, molluscs, aquatic reptiles, amphibians, waterbirds and water-associated mammals. Includes *Crocodylus niloticus, Hippopotamus amphibius, Trichechus senegalensis, Aonyx capensis, Hydrictis maculicollis, Herpestes ichneumon, Redunca redunca* and *Tragelaphus spekii.*
2 (n=14)	Highly water dependent, surviving c. 1 day without water.	Moderate/high – strongly associated with permanent water and/or well-watered riparian habitats	Well-watered environments with reliable permanent surface water and associated riparian or wetland habitat	*Bos primigenius; Connochaetes gnou; Connochaetes taurinus; Erythrocebus patas; Felis Chaus; Hippotragus equinus; Kobus ellipsiprymnus; Kobus kob; Loxodonta africana; Pelorovis antiquus; Potamochoerus porcus; Syncerus caffer; Thryonomys swinderianus; Tragelaphus scriptus.*
3 (n=16)	Moderate dependency – regular access to drinking water required, but capable of ranging away from water for 2 to 3 days.	Low/moderate – not dependent on aquatic habitat but typically occurs in landscapes containing accessible water	Savanna/grassland environments with dispersed but reliable surface-water sources	*Acinonyx jubatus; Ceratotherium simum; Damaliscus lunatus; Diceros bicornis; Diceros bicornis/Ceratotherium simum; Gazella rufifrons; Giraffa camelopardalis; Hyaena hyaena; Hystrix cristata; Ourebia ourebia; Panthera leo; Phacochoerus aethiopicus; Phacochoerus africanus; Rhinocerotidae indeterminate; Taurotragus derbianus; Varanus exanthematicus.*

4 (n=16)	Low dependency – able to tolerate extended periods without drinking or utilise seasonal/ephemeral water	Low – no dependence on permanent aquatic or riparian habitat	Dry savanna and semi-arid environments, where water may be seasonal, ephemeral or widely dispersed	*Alcelaphus buselaphus; Coronella girondica; Equus africanus; Eudorcas thomsonii; Gazella cuvieri; Gazella dama; Gerbilliscus robustus; Ictonyx striatus; Lepus capensis; Meriones shawi; Nanger soemmerringii; Paraechinus aethiopicus; Struthio camelus; Taurotragus oryx; Vulpes pallida; Xerus erythropus.*
5 (n=18)	Very low dependency – highly adapted to water scarcity, capable of surviving with little or no direct drinking water	Very low/none – independent of permanent surface-water habitat	Arid/desert environments, including stony plains and landscapes with little or no permanent surface water	*Addax nasomaculatus; Ammotragus lervia; Centrochelys sulcata; Cerastes cerastes; Ctenodactylus gundi; Felis margarita; Gazella dorcas; Gazella leptoceros; Gerbillus mauritaniae; Gerbillus pyramidum; Ictonyx libycus; Jaculus jaculus; Madoqua saltiana; Nanger granti; Oreotragus oreotragus; Oryx dammah; Vulpes rueppelli; Vulpes zerda.*

Table 1. *Classification of faunal taxa according to the Water Dependency Index (WDI), based on physiological water requirements, habitat associations and hydro-ecological characteristics. WDI values range from 1 (taxa associated with permanent aquatic or wetland environments) to 5 (taxa adapted to arid environments with minimal dependence on surface water). The full species list is presented in table S1.*

We also examine the relationship between hydrology and faunal diversity. Because water availability influences habitat suitability, resource availability and ecological niches, species richness provides an additional measure of the capacity of local environments to support diverse faunal communities. To compare hydrological and faunal indicators of wetness directly, we use the hydrological radiocarbon dates to reconstruct the latitudinal distribution of hydrological activity through time, plotting mean calibrated ages as a kernel density surface alongside the mean WDI of individual site phases. We then quantify the relationship between hydrological intensity and mean WDI using Pearson's correlation coefficient (r).

3.4 Rainbelt model comparison

Our data are sparsely spread when considering both the spatial and temporal range of the study, and therefore statistical power can be leveraged if it is reasonable to aggregate data longitudinally across latitude. Historic monthly precipitation records indicate that the WAM and Westerlies both produce broadly horizontal arid/wet boundaries, with seasonal shifts in these boundaries moving north/south (Fig S1). Late Quaternary climate simulations indicate that while the intensity and extent of major circulation systems varied with orbital forcing and glacial–interglacial cycles, their broad spatial organisation remained relatively stable over the last 800 ka [57]. Thus, the longitudinal similarity in historic rainfall offers some support for a similar structure during the Holocene. We explored this further by constructing a statistical model of two weather systems (Westerlies and WAM) as Gaussian shaped bands of rain, with parameters allowing each rain band to advance and decline at any speed and in any direction. The northern rain band represents the Westerlies, and the Southern rain band represents the WAM. This generated a 2D probability density surface constantly changing through time. By using the georeferences and calibrated radiocarbon dates of each empirical palaeohydrological sample as a proxy for the presence of rainfall, we then calculated the probability of the surface at each of the 1099 empirical points. Overall, this provided the model likelihood (for any particular set of parameter values), given the

palaeohydrological data. Using this framework we then performed a search of parameter space to identify the maximum likelihood parameter values. We compared nine nested models of varying complexity (from 4 to 10 parameters), including two models that excluded the northern rain belt (all rain coming from the WAM), and formally compared them using the Bayesian Information Criterion (BIC) which balances goodness of fit (Likelihoods) against model complexity (number of parameters) to avoid overfitting.

4. Results

4.1 Palaeohydrological features

The palaeohydrological mapping (Fig. 1) illustrates extensive hydrological networks that developed across the Sahara during more humid periods, creating a landscape rich in rivers and lakes that would have provided important habitats and resources for animal and human populations. In total, we mapped 531,520 km of palaeodrainage and 11,996 individual lakes, with a combined surface area of 341,277 km², equivalent to approximately 3.7% of the Sahara. Although most lakes were relatively small, several were vast, including Megalakes Chad and Timbuktu in the southern Sahara [58].

These hydrological features were unevenly distributed across the region. In the eastern Sahara, river systems predominate and lakes are generally small and comparatively sparse. By contrast, the central Sahara contains a broad zone of greater lake abundance and size, extending from Megalake Chad in the south to the Chotts Megalake in the north. Further concentrations of lakes occur in the north-western Sahara, immediately south of the Atlas Mountains, and in the southern Sahara north of Megalake Timbuktu. Together, these spatial differences reveal substantial regional variation in the character and density of surface-water environments across the humid Sahara. However, Fig. 1 should not be interpreted as representing a single hydrological configuration. Most of the mapped lakes have not been ground-truthed, or directly dated, meaning that their precise periods of existence and longevity remain unknown. The map therefore represents the cumulative spatial extent of known and reconstructed surface-water features over the last 7-8 million years, rather than evidence that all rivers and lakes were active simultaneously.

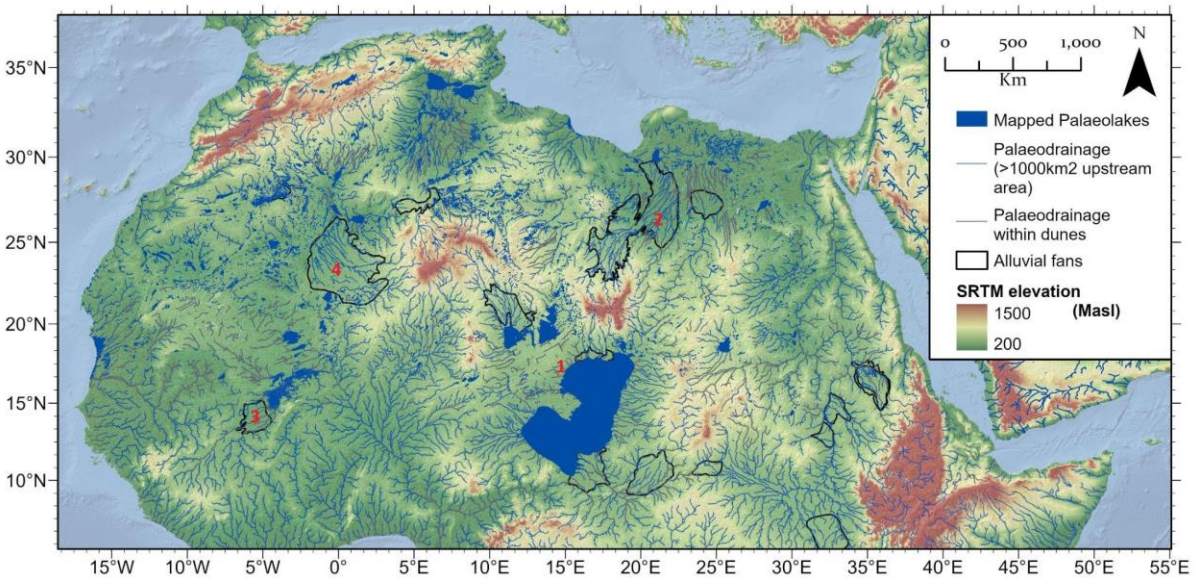

Figure 1. *Distribution of major palaeohydrological features across the Sahara over the last 8 million years. Mapped palaeolakes (blue), major palaeodrainage networks (catchments with upstream drainage areas >1,000 km²), palaeodrainage preserved within dune fields, and alluvial fans are shown over a digital elevation model (SRTM). Prominent hydrological systems discussed in the text include (1) the Lake Megachad basin, (2) the Wadi Behar Belama River and fan, (3) the Niger Basin, and (4) the West Ahaggar Mountains fluvial fan.*

4.2 Catchment activation

Using the catchment activation reconstructions, we can identify the extent of lakes and rivers active during the Holocene. Figure 2 shows that catchment activation was widespread across the Sahara between c.10ka and 4ka, with only limited areas of central and northern Algeria, northern Mali and Mauritania, and eastern and western Libya showing little or no evidence of hydrological activity. Against this widespread background, several regions show particularly persistent or repeated activation through the Holocene, including catchments extending well north of 25°N. Importantly, these do not appear as isolated hydrological hotspots, but form geographically coherent chains that correspond to potential trans-Saharan hydrological corridors. In the central-eastern Sahara, repeated activation links the Lake Mega-Chad basin with the Tibesti highlands and the Wadi Behar Belama (number 2 in Fig. 1; Fig. 2) that drains the northern Tibesti towards the Mediterranean and was activated repeatedly throughout the Holocene as shown in Fig 2. Further west, repeatedly activated catchments associated with the Niger Basin and West Ahaggar Mountains form part of a broader central Saharan network, potentially connecting the Sahel with the Ahaggar and northwards to Mediterranean North Africa. In the eastern Sahara, repeated activation is also evident across several Nile sub-catchments, forming a comparatively continuous north–south hydrological axis through Sudan and Egypt. Activated catchments extending westwards from the Nile towards the Nubian Desert, Gilf Kebir and Uweinat regions may also have provided lateral connections between the Nile Valley and the interior Saharan drainage networks. These patterns correspond closely with the major megalake basins, palaeodrainages and alluvial systems previously identified by Drake et al. [30] particularly Lake Mega-Chad, the Niger Basin and the West Ahaggar fluvial fan (numbers 1, 3 and 4 in Fig. 1, respectively). Collectively, the spatial continuity and repeated activation of these catchments suggests

that Saharan hydrological connectivity may have been structured around a series of persistent riparian corridor networks and hydrological hubs, rather than isolated episodes of localised humid conditions.

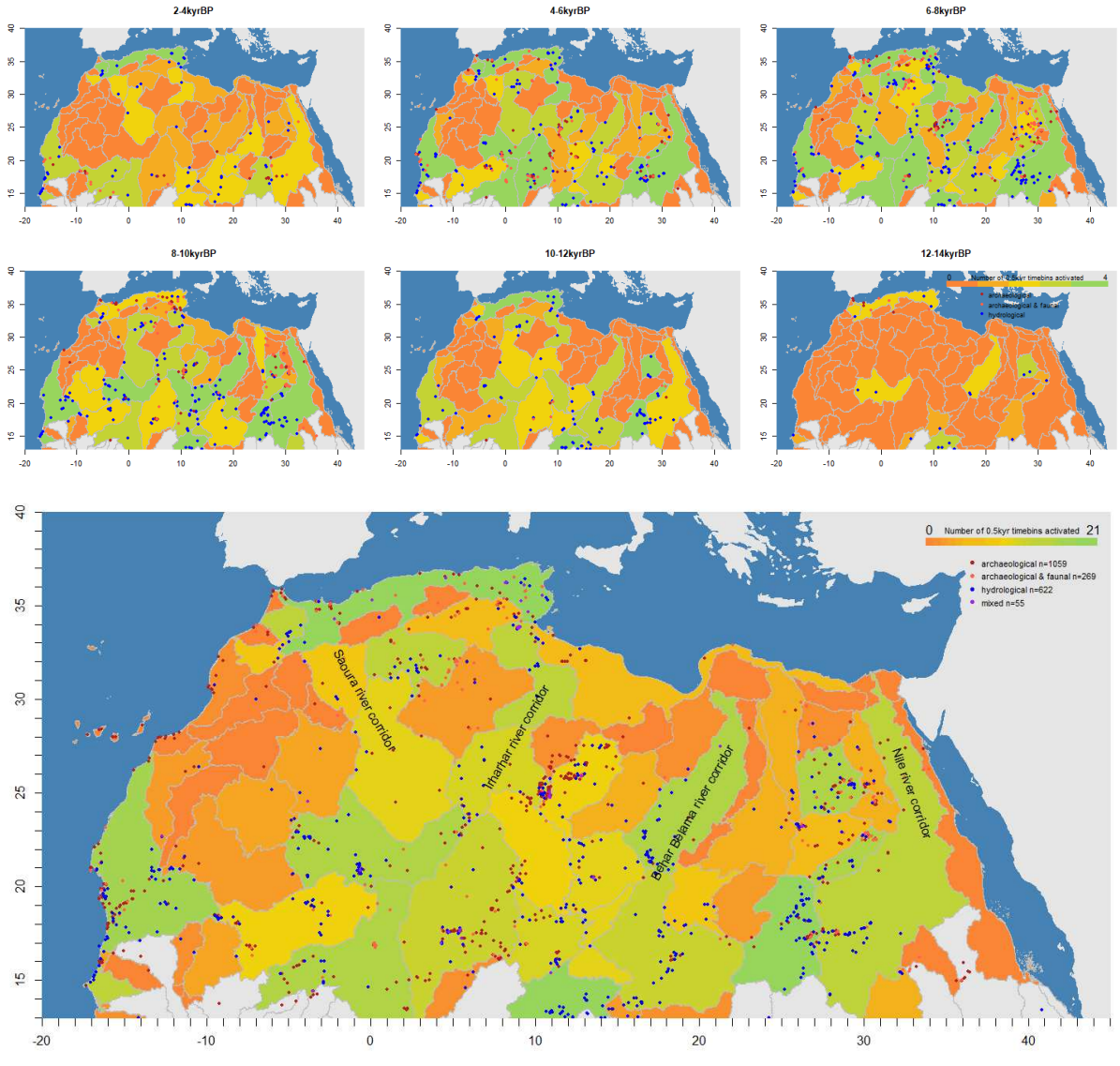

Figure 2. *Reconstruction of Holocene hydrological activation across the Sahara showing HydroBASINS level 4 catchments between 14 and 2 ka BP, calculated from hydrologically associated radiocarbon dates. Catchment colour indicates the number of 500 yr time intervals in which hydrological activity is recorded (activation count).*

Whilst this catchment activation reconstruction provides a proxy for spatial and temporal variation in wetness, the spatial component has several limitations. Firstly, rainfall in any part of a catchment will flow to the same accumulation point (such as a river or lake), allowing the direct inference that water at the accumulation point came from somewhere upstream in the catchment. However, in deserts, catchments are typically characterised by endorheic basins hosting one or more terminal lakes rather than the throughput to ocean outlets more typically seen in wetter climes. In such cases multiple drainage systems terminate in the same depression, and it is possible for rainfall to have only occurred in one part of a catchment and still generate a lake at its core.

Likewise, although a dated river provides evidence of flow somewhere upstream, it cannot be determined how far upstream it originated.

The Saoura River provides a useful example of the difficulties involved in translating evidence for palaeohydrological activity into the spatial distribution of past rainfall. Originating in the Atlas Mountains, the river extends approximately 835 km southwards into the Sahara, terminating in the Reggane Basin (Fig. 3A). Historical records demonstrate that floodwaters can travel considerable distances downstream: between the years 1900 and 1957, 33 floods travelled >200 km, 13 >300 km, six >400 km, five >500 km and one >800 km [59] Sebkha el Melah, approximately 560 km downstream, fills during sufficiently large flood events (Fig. 3B); Landsat imagery records filling in 1994, 2010–11, 2014–16 and 2024–25.

Radiocarbon dates from freshwater molluscs, marsh deposits, marl, organic sediments and calcareous tufa record repeated palaeohydrological activity along the Saoura during the Late Pleistocene and Holocene (Fig. 3C). The SPD shows episodic activity prior to ~11 ka BP, followed by substantially greater activity during the African Humid Period, with the highest concentration of dates between ~6.5 and 4.9 ka BP. Hydrological activity subsequently declines towards the Late Holocene.

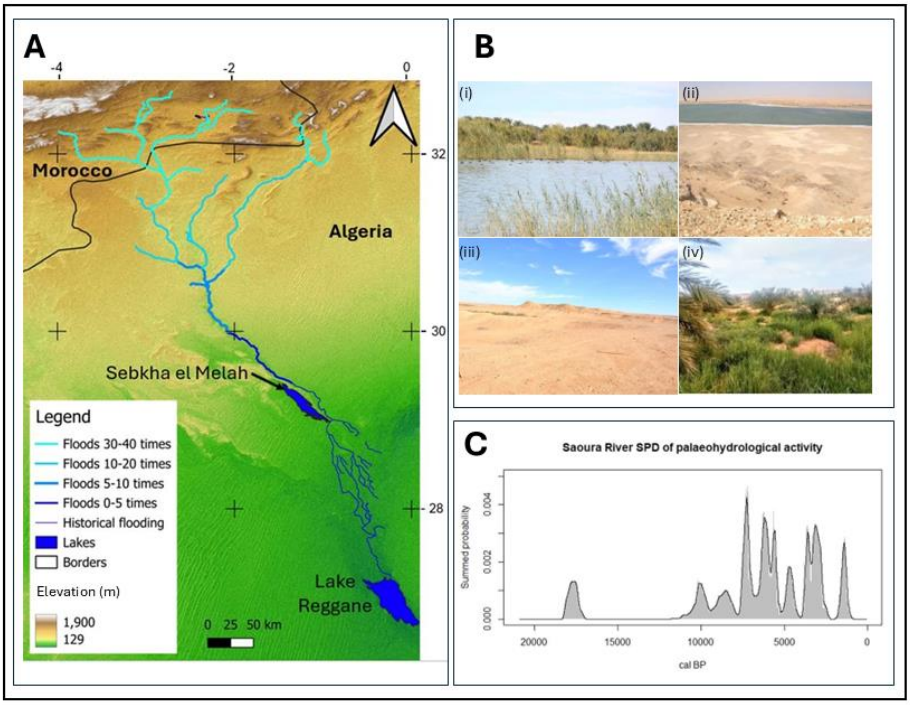

***Figure 3**. Modern and palaeohydrological activity of the Saoura River system. **(A)** Saoura River drainage network extending from the Atlas Mountains into the Sahara to Lake Reggane, with river reaches coloured according to the frequency and downstream extent of historical flood events reported by Dumont (1988). **(B)** Present-day environments (2016-2019) associated with the Saoura system: (i) General view of Southern side of Sebkhat El Melah lake, (ii) General view of the Northern basin, (iii) Palm grove neighboring the lake (iv) Reg biotope in the periphery of the lake. **(C)** Summed probability distribution (SPD) of 23 calibrated radiocarbon dates from palaeohydrological records associated with the Saoura River, showing episodic Late Pleistocene activity and increased hydrological activity during the African Humid Period. Panel B adapted from Arachnid*

fauna of the Sebkhat El Melah-Ramsar site in the Sahara Desert of Algeria (2022), Revista Ibérica de Aracnología, 40, 165–169 [60].

4.3 Rainbelt model comparison

Comparison of the Bayesian Information Criterion (BIC) of nine nested rainbelt models provides independent support for the broad latitudinal structure evident in the palaeohydrological data. Models incorporating both a southern and northern rainbelt were better supported than those in which all hydrological activity was attributed to a single southern rainbelt (Table S2, models 4 and 5), indicating distinct contributions from the WAM and a northern precipitation system driven by the westerlies. The three models (Table S2, models 10, 9a, 9b) that gave parameter freedom to the southern belt to vary in any direction from 0° (moving North-South) to 45° (Northeast - Southwest) all favoured an angle of 0° in their maximum likelihood parameter searches. The overall best supported model (model 9c, lowest BIC) had the southern belt direction fixed at 0°, whilst its northern rainbelt followed a slightly South-southeast trajectory of -9.45° from horizontal (Fig. 4), thus broadly replicating the zonal structure and seasonal rainbelt directions observed in modern rainfall (Fig S1). The model also provides quantitative estimates of Holocene rainbelt dynamics. The northwards expansion of the WAM accounted for 82% of modelled rainfall, moving at 0.00058° yr^{-1}, c. 6.4km per century, and maximum northward extent occurring at approximately 7790 BP before subsequent retreat. The MWP, driven by the westerlies accounted for the remaining 18% of modelled rainfall, moving at a slower rate of 0.00028 ° yr^{-1} , c.3.1km per century (Table S2). These estimates indicate that the two rainfall systems made unequal contributions to Saharan wetness and provide an independent temporal constraint on the expansion and contraction of humid conditions across the Sahara. These results also provide support for aggregating the palaeohydrological and faunal records longitudinally for subsequent analysis of their dominant latitudinal structure, particularly where drawing inferences about the northern extent of the WAM.

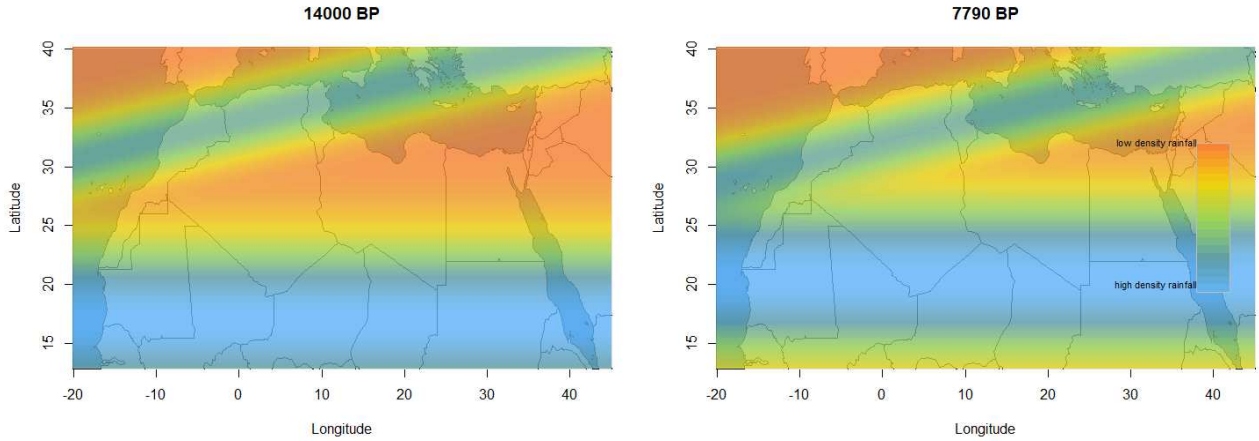

Fig 4*: Rainbelt model 9c best fits the palaeohydrologically associated radiocarbon dates used a proxy for date and location of rainfall (Table S1, lowest BIC), supporting a predominant rainbelt from the south (WAM) moving North, and a smaller rainbelt from the north (MWP) moving approximately South-southwest (-9.45° from horizontal). The belts reach their maximum extent at 7790BP before reversing direction.*

4.3 Bioclimatic analysis from faunal remains

The distribution of fauna shows a pronounced latitudinal structure (Fig. 5). Between 14°N and 25°N, all five WDI classes are represented, with water-dependent taxa (WDI 1–3) occurring frequently alongside more arid-adapted species. Faunal richness is particularly high between 15°N and 19°N, where the 1° latitude bands contain an average of 79 (min 57 and max 91) species across all phases, and individual site phases frequently have low mean WDI values, indicating assemblages containing a substantial component of diverse water-dependent fauna. North of 25°N, both richness and the representation of water-dependent taxa decline markedly, producing a broad gap in both species diversity and fauna that require regular access to water. There is a marked absence of sub-Saharan fish species north of 25.14°N (e.g. Tilapinii and Claridae), suggesting the WAM response was significantly weakened in these northern regions as to negate the dispersal of fully water-dependent sub-Saharan species beyond this limit.

There are, however, several important exceptions to this broader pattern, which providing additional, independent evidence for spatially discrete riparian environments within the otherwise arid belt. The first concerns the occurrence of WDI = 1 taxa between 25°N and 33°N. At Ti-n-Torha (25.14°N), in the Tadrart Acacus region of Libya, several freshwater fish species have been identified. Although the main Irharhar drainage system lay further west, a broader network of palaeochannels and alluvial valleys extended across the central Saharan massifs, including the Tadrart Acacus. Wadi Ti-n-Torha was also supplied by groundwater-fed springs emerging from the surrounding sandstone formations, potentially sustaining localised aquatic habitats even when regional surface-water availability was limited. Further north, the only other occurrence of WDI = 1 taxa within this latitudinal belt is recorded at Zmeilet el-Barka (29.12°N), Algeria, within the Saoura River corridor. This assemblage contains taxa spanning all five WDI categories, including arid-adapted species such as oryx and gazelle alongside freshwater molluscs, including *Melanoides tuberculata*, which can inhabit freshwater and brackish environments. The WDI = 3 occurrence at this latitude (Fig. 5) also derives from this site. Together, these records suggest that localised aquatic habitats persisted within otherwise predominantly arid landscapes, consistent with the presence of riparian environments sustained by groundwater discharge and/or episodic river activation. Additional exceptions occur further east, where isolated elephant remains (WDI = 2) have been recorded at 27.5°N within the Wadi Behar Belama corridor and at Haua Fteah (32.9°N), near its northern extent on the Mediterranean coast. Outside of the Wadi Behar Belama corridor, WDI = 2 taxa are absent between approximately 24.5°N and the Mediterranean margin. The faunal discontinuity is particularly pronounced between 30°N and 32°N (Fig. 4), where only WDI=4 taxa are found. These includes species such as ostrich (*Struthio camelus*), and barbary sheep (*Ammotragus lervia*), which inhabit savanna and desert environments and possess physiological and digestive adaptations that allow them to obtain much of their water from forage [61, 62].

Collectively, these distributions indicate a marked northward transition from relatively diverse faunal assemblages containing numerous water-dependent taxa to much sparser assemblages dominated by species adapted to limited surface-water availability. The restricted occurrence of water-dependent taxa along reconstructed drainage systems further supports the interpretation of a persistent arid belt traversed by spatially

discrete riparian corridors, rather than a continuously humid landscape across the northern Sahara. Importantly, the co-occurrence of xerocolous and water-dependent taxa at lower latitudes should not be interpreted as evidence for arid conditions. Rather, it likely reflects the heterogeneous nature of Saharan landscapes during humid phases, where lakes, wetlands and riparian corridors occurred within broader savanna and semi-arid environments, supporting species with contrasting water requirements within the same regional species pool. In contrast, northern assemblages dominated by xerocolous taxa, with few or no species requiring regular access to surface water, suggest more spatially restricted water availability. Rather than the widespread humid savanna environments inferred farther south, these assemblages are more consistent with heterogeneous desert-margin landscapes comprising dry savanna, steppe and localised riparian environments. Previous analysis of the zoogeography of North Africa [30] suggested that savanna species such as elephant (*Loxodonta africana*) and giraffe (*Giraffa camelopardalis*) could have extended further north up to 29°N. However, these records are based on rock art depictions, which introduce a number of potential biases, including dating uncertainty, and whether the cultural perceptions of the Holocene artists were inspired by the local macrofauna, or if the art served the formation and recursive maintenance of ancestral memory. Such remote mapping of cultural geography has been observed ethnographically across many desert environments [63-65].

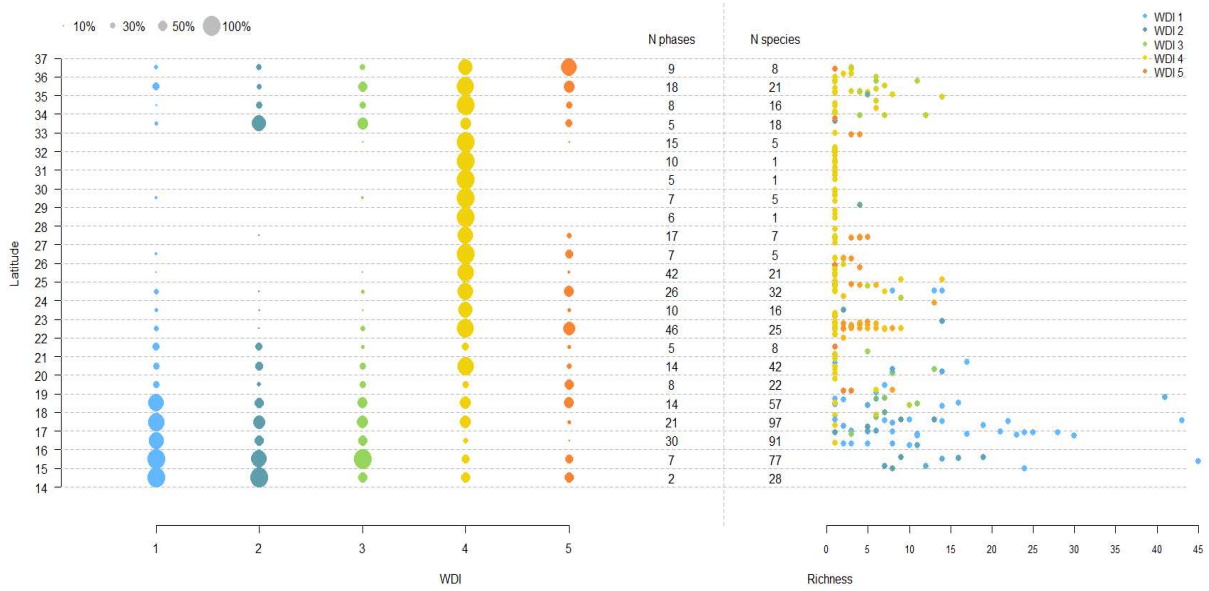

Figure 5. *Latitudinal distribution of key ecological taxa assigned a Water Dependency Index (WDI) value. WDI values are represented by colour. Left: Proportion of all site phases within a 1 degree band that contain taxa assigned a WDI value. Right: Richness (number of different species) at all 332 site phases that contain taxa with WDI values, coloured by mean WDI value weighted by NISP.*

Importantly, the bioclimatic inferences drawn from the archaeozoological record agree with other anthropogenic records. Few archaeological sites have been identified between 28°N and 32°N, and those that are known consist predominantly of lithic scatters, with faunal remains occurring only rarely. Typically dating to the Epipalaeolithic, such sites have been documented around Ouargla in Algeria and along the Jebel Nafusa in Libya. The limited nature of these assemblages suggests highly ephemeral occupation, likely associated with

mobile hunter-gatherer groups moving through the region. This dearth of archaeological material is unlikely a result of differential taphonomy as deflation of deposits and desiccation of organic remains are a problem for preservation across the entire Sahara, not just in northern latitudes. Equally, soil acidity shows no latitudinal structure [66] that would explain the differential evidence of occupation.

4.4 Hydro-ecological correspondence

Although we cannot identify the precise source of precipitation within individual hydrological catchments, we can examine correspondence between the archaeological, faunal and hydrological records to better constrain where rainfall generated conditions capable of supporting sustained surface water, viable habitats and human occupation. Figure 5 maps the evidence for human presence during the AHP alongside the activated catchments, with 18 of the 23 500yr timeslices showing statistically significant correlation between catchments being hydrologically activated and containing archaeology ($p<0.05$ using Jaccard test). In particular, there is good correspondence between the evidence for human occupation and the re-activated catchments that connect the Niger basin to the Saoura River via the rivers draining from the Hoggar mountains which also connect to the Chotts basins via the Irharhar River. These hydrological connections indicate corridors across the Sahara that likely occurred when the WAM was more intense [67-70]. The evidence from these archaeological sites, however, are sparse and likely represent ephemeral campsites resulting from high mobility, rather than permanent occupation sites.

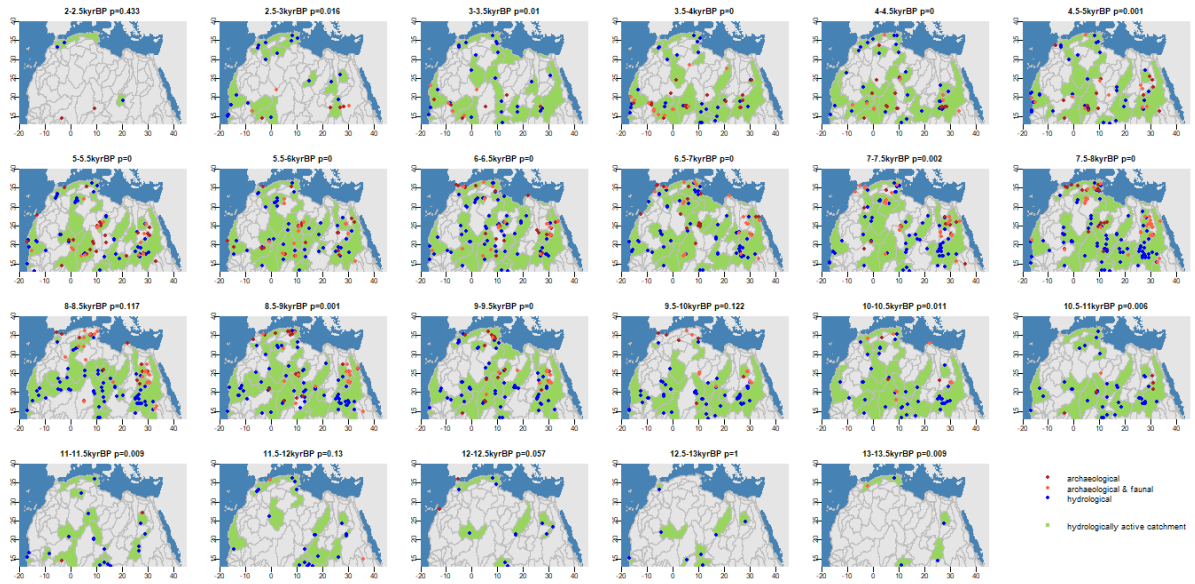

Figure 6. *Reconstruction of Holocene hydrological activation across the Sahara showing HydroBASINS level 4 catchments in 500 yr time slices between 13.5 and 2 ka BP. Green regions indicate catchments in which hydrological activity is recorded (blue dots). Red and orange dots indicate archaeological evidence of human presence. P-values in each timeslice indicate the statistical significance of spatial correlation between catchments being hydrologically activated and catchments containing archaeology, using the Jaccard Index (R package Jaccard), showing substantial similarity between both independent datasets, with 18 of the 23 timeslices showing statistical significance ($p<0.05$).*

In addition to incorporating hydrological radiocarbon dates into the catchment activation analysis, we examine their spatiotemporal distribution using a kernel density surface generated from the weighted mean calibrated ages (Fig. 7). This enables direct comparison with the faunal Water Dependency Index (WDI) and reveals a high density of hydrological dates during the early Holocene (11–7 ka), extending northwards to approximately 22°N. Although the available faunal assemblages generally contain water-dependent taxa (low WDI values), there is a marked scarcity of archaeological faunal records at these latitudes between 11 and 8 ka. This apparent gap may partly reflect taphonomic and sampling biases associated with the expansion of lakes and wetlands during the early African Humid Period. Rising lake levels and increased floodplain sedimentation could have submerged, buried or reworked archaeological deposits, reducing the visibility of early Holocene occupation surfaces. Similar processes have been documented at Gobero in Niger, where archaeological sites were periodically submerged during Holocene lake highstands [71]. Alternatively, extensive wetlands may have influenced settlement distributions, concentrating human activity along elevated shorelines and other favourable locations. The scarcity of early Holocene faunal records should therefore not necessarily be interpreted as evidence for limited occupation or reduced faunal diversity.

From approximately 7 ka, the density of hydrological dates declines markedly, consistent with a regional transition towards drier conditions. Nevertheless, the continued occurrence of low WDI values suggests that habitats supporting water-dependent fauna persisted south of approximately 22°N throughout the Holocene. The broad spatiotemporal pattern of hydrological activity is consistent with that identified by Lézine et al. [3], reflecting the overlap between the underlying datasets. However, our analysis extends the geographical coverage north of 28°N and integrates independent faunal evidence, providing additional insight into the spatial heterogeneity of Holocene surface-water availability.

Importantly, Fig. 7 reveals a striking and persistent latitudinal contrast in faunal distributions. Throughout the Holocene, assemblages north of approximately 22°N are predominantly composed of arid-adapted taxa, including during the early and middle Holocene when hydrological records indicate more extensive surface-water availability further south. This suggests that the ecological transition around 22°N was not simply a consequence of mid-Holocene aridification but characterised much of the Holocene. Occurrences of more water-dependent taxa further north are geographically restricted, rather than distributed continuously across this latitudinal belt as discussed above. These are concentrated particularly in the Tadrart Acacus Mountains of southwestern Libya, including the sites of Takarkori and Ti-n-Torha. Further north, the two localised exceptions, are the isolated elephant occurrence along the Wadi Behar Belama system, and the freshwater molluscs from the Saoura river region. There is a marked absence of sub-Saharan fish species north of 25.14°N (e.g. Tilapinii and Claridae), suggesting the WAM response was significantly weakened in these northern regions as to negate the dispersal of fully water-dependent sub-Saharan species beyond this limit.

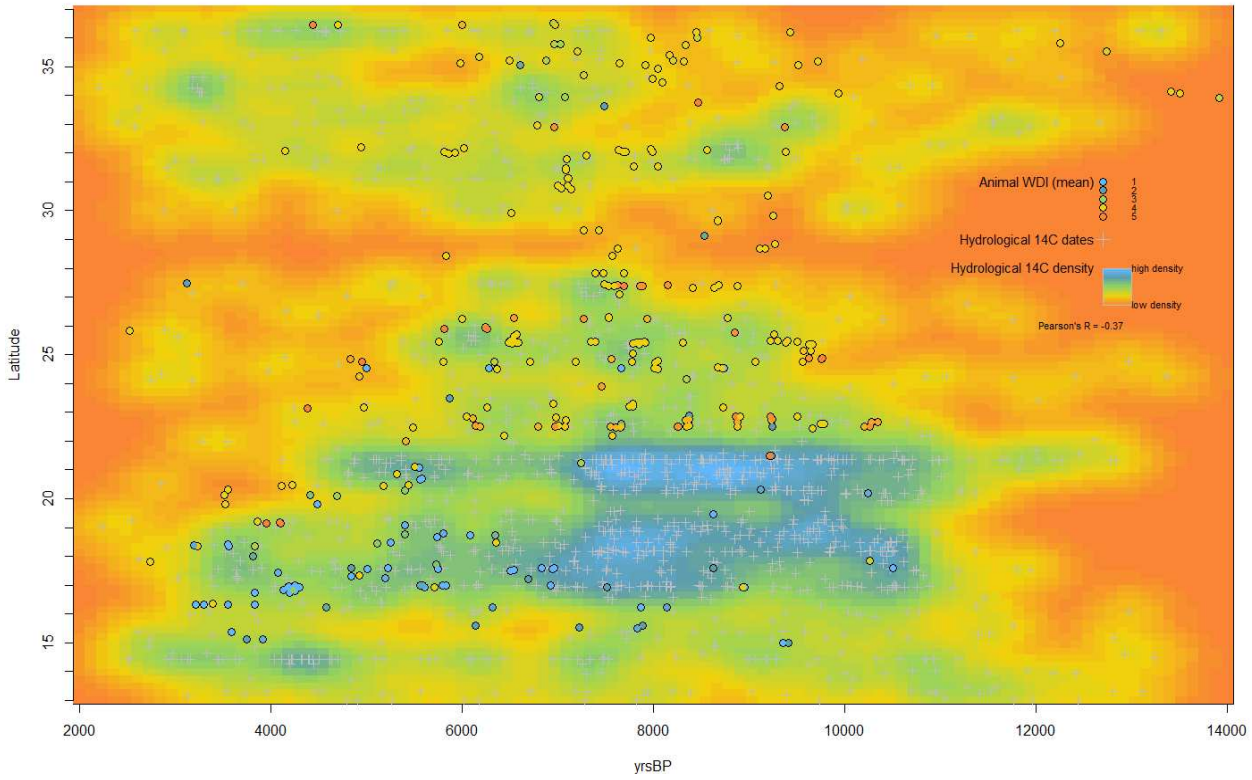

***Figure** 7. Kernel density interpolation of hydrological intensity through time, generated from 1233 radiocarbon dates directly associated with hydrological activity (grey crosses). The overlayed Water Dependency Index (WDI) of faunal remains from 332 site phases are correlated with the kernel density values (Pearsons' R = -0.374, p=2.6e^{-12}). Note the blue dot at 8000 BP at ~29°N is the diverse faunal record from* Zmeilet el-Barka, along the Saoura river corridor.

Comparison of the hydrological and faunal records therefore reveals broad agreement in the spatial and temporal pattern of Holocene wetness, but also important differences between the two proxies. Hydrological intensity and WDI are significantly correlated (Pearson's r = −0.374, p=2.6e^{12}; Fig. 7), with greater hydrological intensity corresponding to *lower* (hence the negative correlation) WDI values, or greater water dependency. However, the moderate strength of this relationship reflects differences in what the proxies record and their spatial and temporal coverage. Hydrological dates provide direct evidence for the activation of lakes, rivers and wetlands, whereas faunal assemblages indicate whether local landscapes supported animal communities with differing dependencies on surface water. Crucially, Fig. 7 reveals a clear latitudinal zone where evidence for sustained humid ecosystems is absent at 29°N throughout the Holocene. For much of the Holocene, this arid belt spreads across almost 3° of latitude between 28°N and 31°N and is only reduced to a narrower 1° latitudinal width (c. 1000km) for a short period of time, between c. 8ka and 6ka. Beyond 22°N, however, evidence for surface water is clearly reduced and we can observe a clear delineation in both the hydrological date density and the WDI values. This abrupt latitudinal boundary indicates a rapid decline in the WAM response north of 22°N. Above this, smaller regional ecologies which supported more water-dependent species occur only in sporadic areas as a consequence of complex interactions of groundwater recharge, and orographic uplift in mountain regions.

4. Discussion

Deterministic models of Holocene greening across North Africa have significantly improved over recent years, incorporating dynamic dust, vegetation feedbacks, and moisture recycling from lakes and wetlands [12, 37-39, 46]. The timing of Saharan humid phases broadly follows changes in Northern Hemisphere summer insolation, with enhanced early Holocene insolation strengthening land–ocean temperature gradients and driving northward expansion of the WAM, followed by progressive weakening as insolation declined. However, the magnitude and spatial extent of this response remains debated. Whilst 'orbital-only' models typically stalled the WAM extent at ~17–20°N, most coupled climate simulations extend the monsoon rain belt northward to ~26°N. Previous attempts at model validation have typically relied on coarse temporal and spatial datasets, notably vegetation reconstructions from pollen [2, 27, 72] and leaf wax biomarkers [1, 73]. However, different proxy systems record different components of the climate–environment response, contributing to apparent disagreement in reconstructions of Saharan greening. For example, Thompson et al. [74] demonstrated that discrepancies between dust, pollen and leaf wax records partly reflect differences in proxy sensitivity, with some archives responding primarily to precipitation and atmospheric transport processes, while others record vegetation structure and ecological change. This distinction is critical when defining the spatial extent of the "Green Sahara". Depending on whether exclusive, or non-exclusive taxa are used, pollen records suggest the Sudanian group, which require rainfall rates between 500 and 1500 mm/year, expanded either to just 14-16°N or 25°N respectively during the early Holocene when using the 0.85 isoprobability which delineates the maximum extent zone in which 85% of the samples are included [3]. In contrast, based on leaf wax biomarkers and inferred precipitation rates from ocean core sediment sites, Tierney et al. [1] propose that a seasonal tropical climate dominated most regions of North Africa during the Holocene.

Using an updated and expanded radiocarbon dataset from palaeohydrological sites, combined with a new wetness indicator based on the water-dependence of animal populations hunted by Holocene occupants of the Sahara, we provide new constraints on the ecological expression of WAM expansion. Our results suggest that conditions capable of sustaining water-dependent faunal communities were rare beyond ~28°N, with evidence for a reduction in effective moisture north of ~22°N in lowland areas. Similarly, neither the faunal data nor palaeohydrology provides strong evidence for widespread Mediterranean-influenced humid environments south of ~29°N resulting in a hydro-ecological transition zone that for much of the Holocene covered a ~3° latitudinal band. Even at the maximum extent of both the Mediterranean winter precipitation system and the intensified summer monsoon, a 1° belt of aridity persisted across all longitudes.

However, the persistence of this latitudinal zone of reduced effective moisture as suggested by the faunal remains, contrasts with the catchment analysis which indicates hydrological corridors that intermittently connected humid regions across North Africa. Large drainage systems originating outside the hyper-arid core of the Sahara acted as spatially restricted but ecologically important riparian pathways, where episodic flooding, shallow groundwater and residual pools supported localised vegetation and water availability. Such systems would not be resolved by regional precipitation reconstructions but may have provided corridors for the movement of humans and fauna across otherwise unsuitable landscapes.

The Saoura River provides a clear example of this process. Originating in the Atlas Mountains, the Saoura extends ~835 km southwards into the Sahara. As demonstrated by the historical flood record (Fig. 3A), floodwaters can propagate hundreds of kilometres downstream under modern climatic conditions, with events exceeding 500 km occurring approximately once per decade and exceptional floods extending almost the entire length of the system [59]. The repeated filling of Sebkha el Melah, ~560 km from the headwaters, provides further evidence that substantial surface-water resources can develop deep within the desert because of rainfall occurring far upstream. Importantly, our palaeohydrological chronology indicates that this connectivity was substantially enhanced during the Holocene. Radiocarbon evidence supports repeated fluvial and wetland activity along the Saoura, with particularly pronounced activity during the African Humid Period and a concentration of dates between ~6.5 and 4.9 ka BP (Fig. 3C). The Saoura therefore demonstrates that substantial hydrological connectivity could extend across regions in which our wider reconstruction indicates comparatively limited effective moisture. A similar mechanism is evident in the Wadi Behar Belama system, a major northward-draining corridor originating in the Tibesti Mountains and extending across the central Sahara (SI - Wadi Behar Belema and Serir Tibesti Fluvial Fan Case study).

Satellite imagery reveals an extensive network of abandoned channels forming the Serir Tibesti fluvial fan, indicating repeated activation and avulsion of drainage pathways across the Sirte plains [30]. Groundwater geochemistry from the Sirte Basin provides evidence for Holocene recharge from this system, with radiocarbon ages of ~7800 BP indicating significant flow more than 900 km from the Tibesti headwaters [75]. Late Holocene elephant remains dated to ~3500 BP [76] provide further support that these corridors remained intermittently viable, allowing mobile species to exploit episodic water and vegetation resources in a manner comparable to modern desert-adapted elephants using ephemeral river systems in the Namib. Collar tracking on these elephants has, for example, indicated that adult males can have a large home range of 2881 to 12800 km^2 in such arid environments, likely due to them searching for females in oestrus far outside their normal home ranges [77]. Similarly, elephant remains from Haua Fteah demonstrate that the northern margins of Africa supported water-dependent megafauna during periods of enhanced humidity, reflecting ecological connectivity between Mediterranean landscapes and the wider Saharan interior. This interpretation is independently supported by recent phylogeographic and species-distribution modelling, which identifies a Central Saharan mesic corridor connecting the Mediterranean and Sahel through a series of Saharan highland refugia during humid phases [78].

These examples help reconcile the apparent discrepancy between widespread hydrological activation identified through catchment reconstruction and the more restricted extent of humid environments inferred from ecological indicators. While Saharan greening was primarily controlled by the latitudinal expansion and contraction of major rainfall systems, hydrological connectivity was also strongly shaped by inherited drainage networks. As a result, activated catchments do not necessarily indicate widespread local precipitation or continuous savanna habitats, but may instead reflect water transported from distant source regions through large fluvial systems. Our archaeological data and WDI analysis indicates that these corridors were utilised by mobile water-dependent species and past human populations (Fig. 5 and Fig. 6), although the broader absence of water-dependent fauna outside these hydrological pathways, together with the ephemeral nature of archaeological occupation in these

corridor regions, suggests that these Holocene systems provided only transient windows of connectivity rather than supporting sustained ecological expansion or long-term population establishment across the arid belt.

The timing of the hydro-ecological transition identified here also provides new constraints on the spatial retreat of humid conditions. Our results indicate a marked contraction of wet conditions from ~7790 BP, substantially earlier than the ~5.5 ka BP termination of the African Humid Period inferred from the widely cited northwest African marine dust record [17]. Rather than indicating an earlier termination of the AHP as a whole, this finding is consistent with evidence that Saharan aridification was spatially asynchronous, with drying occurring earlier at higher northern latitudes and progressively later towards the south [79]. Terrestrial records similarly indicate earlier drying; at Selima Oasis in the eastern Sahara, for example, peak humid conditions centred on ~8 ka BP were followed by increasing aridity after ~7 ka BP [80]. Although high-resolution records from Lake Yoa identify a pronounced drought at ~8.2 ka BP, subsequent recovery of humid conditions suggests that this was a relatively short-lived event. The sustained transition in our reconstruction from ~7790 BP may therefore record an early stage in the longer-term contraction of northern Saharan humid environments, rather than either the 8.2 ka event or the final termination of the AHP.

Gaining clarity on the spatial and temporal extent of these Holocene humid conditions has major implications for understanding both regional environmental change and global climate feedbacks. The Sahara is a critical component of the Earth system, influencing atmospheric circulation, dust emission, and oceanic biogeochemistry. While the timing of North African humid phases is ultimately paced by changes in Northern Hemisphere summer insolation, our results demonstrate that the ecological expression of this forcing was spatially complex. The apparent differences between proxy reconstructions reflect, in part, the different components of the climate–environment system that they record: leaf wax and dust records integrate broad-scale hydroclimatic change, pollen reflects regional vegetation responses [74], palaeohydrological archives identify the activation of drainage networks, and faunal assemblages provide constraints on the persistence of ecologically viable habitats. The persistence of reduced effective moisture north of ~27°N, even under peak summer insolation forcing, therefore demonstrates that orbital forcing alone does not determine the spatial extent of ecological greening. Instead, the environmental expression of humid periods reflects the interaction between large-scale atmospheric circulation, vegetation and dust feedbacks, groundwater and fluvial systems, and inherited landscape structure.

Furthermore, this distinction between regional aridity and localised resource availability has important implications for understanding both earlier hominin dispersals across North Africa and future population movement in response to contemporary climate change. Recent evidence from Guefaït-4 in Morocco indicates that hominins occupied heterogeneous landscapes in which wetlands and resource-rich habitats occurred alongside seasonally arid environments [53]. Our results suggest that such spatial heterogeneity may also have facilitated movement at much larger scales, consistent with phylogeographic evidence identifying connectivity between Mediterranean and sub-Saharan mesic populations through Central Saharan highland refugia during humid phases [78]. Although our Holocene reconstruction cannot identify earlier hominin routes directly, it demonstrates how hydrological connectivity could periodically link suitable habitats across persistent zones of aridity.

This spatial perspective is also relevant to contemporary climate adaptation, as increasing heat, drought and water scarcity are expected to reshape the distribution of viable livelihoods and influence patterns of population mobility across North Africa [81]. As in the past, future population responses are therefore likely to depend not simply on regional climatic trends, but on the spatial distribution and connectivity of water, productive landscapes and other critical resources.

Future work should expand this terrestrial proxy coverage, especially in the central and northern Sahara, and integrate it with palaeoceanographic, isotopic, archaeobotanical, pollen, and speleothem records from adjacent regions. Such multi-proxy syntheses will refine reconstructions of the latitudinal hydrological gradient between the tropics and the Mediterranean and help constrain the phasing and strength of the WAM and Westerlies through time. Using these improved boundary conditions to constrain and validate next-generation Earth system models will further advance understanding of the wider climatic impacts of Saharan greening. Previous simulations have already demonstrated that reductions in Saharan dust emissions and expansion of vegetation can influence atmospheric circulation, tropical rainfall, ITCZ position and remote climate teleconnections. Resolving where greening represented continuous ecosystem transformation versus more spatially restricted hydrological connectivity, and when these different components of the humid landscape began to contract, is therefore essential for understanding the sensitivity of the North African climate system and its wider role in population dispersals and global climate feedbacks.

Acknowledgments

We thank Leverhulme for funding the Green Sahara Project (Grant RPG-2016-115) during which the core data collection was conducted, and the analysis was supported by the synergy project 'COREX: From Correlations to Explanations: towards a new European prehistory', funded by the European Research Council (ERC) under the European Union's Horizon 2020 research and innovation programme (Grant Agreement No. 95138) and the Joined Up Landscapes project, a part of the Maximising UK Adaptation to Climate Change (MACC) programme and jointly funded by UKRI (NERC) and Defra (Award number UKRI1280).

Data availability

All data and code is available at https://github.com/AdrianTimpson/Manning-Green-Sahara-Aridity

Author Contributions

Katie Manning: Conceptualization, Methodology, Visualization, Data curation, Writing, Reviewing and Editing. **Paul Breeze**: Methodology, Visualization, **Nick Drake**: Writing, Reviewing and Editing. **Adrian Timpson**: Methodology, Data analysis, Visualization, Writing, Reviewing and Editing..

Competing Interests

The authors declare no competing interests.

Bibliography

1. Tierney, J.E., F.S. Pausata, and P.B. deMenocal, *Rainfall regimes of the Green Sahara.* Science advances, 2017. **3**(1): p. e1601503.
2. Hély, C. and A.-M. Lézine, *Holocene changes in African vegetation: Tradeoff between climate and water availability.* Climate of the Past, 2014. **10**(2): p. 681-686.
3. Lézine, A.-M., et al., *Sahara and Sahel vulnerability to climate changes, lessons from Holocene hydrological data.* Quaternary Science Reviews, 2011. **30**(21-22): p. 3001-3012.
4. Manning, K. and A. Timpson, *The demographic response to Holocene climate change in the Sahara.* Quaternary Science Reviews, 2014. **101**: p. 28-35.
5. Street, F.A. and A. Grove, *Environmental and climatic implications of late Quaternary lake-level fluctuations in Africa.* Nature, 1976. **261**(5559): p. 385-390.
6. Nicholson, S.E. and H. Flohn, *African environmental and climatic changes and the general atmospheric circulation in late Pleistocene and Holocene.* Climatic change, 1980. **2**(4): p. 313-348.
7. Ritchie, J.C., C. Eyles, and C.V. Haynes, *Sediment and pollen evidence for an early to mid-Holocene humid period in the eastern Sahara.* Nature, 1985. **314**(6009): p. 352-355.
8. Gaetani, M., et al., *Mid-Holocene climate at mid-latitudes: assessing the impact of Saharan greening.* Climate of the Past, 2024. **20**(8): p. 1735-1759.
9. Tiwari, S., et al., *Mid-Holocene El Niño Southern Oscillation variability reduced by northern African vegetation changes in climate models.* Communications Earth & Environment, 2025. **6**(1): p. 675.
10. Tiwari, S., et al., *On the Remote Impacts of Mid-Holocene Saharan Vegetation on South American Hydroclimate: A Modeling Intercomparison.* Geophysical Research Letters, 2023. **50**(12): p. e2022GL101974.
11. Street-Perrott, F., et al., *Global lake-level variations from 18,000 to 0 years ago: A palaeoclimate analysis*. 1989, Oxford Univ.(UK). Geography School.
12. Claussen, M. and V. Gayler, *The greening of the Sahara during the mid-Holocene: results of an interactive atmosphere-biome model.* Global Ecology and Biogeography Letters, 1997: p. 369-377.
13. Claussen, M., et al., *Simulation of an abrupt change in Saharan vegetation in the mid-Holocene.* Geophysical research letters, 1999. **26**(14): p. 2037-2040.
14. Jolly, D., et al., *Biome reconstruction from pollen and plant macrofossil data for Africa and the Arabian peninsula at 0 and 6000 years.* Journal of Biogeography, 1998. **25**(6): p. 1007-1027.
15. Kuper, R. and S. Kropelin, *Climate-controlled Holocene occupation in the Sahara: motor of Africa's evolution.* science, 2006. **313**(5788): p. 803-807.
16. Ehrmann, W. and G. Schmiedl, *Nature and dynamics of North African humid and dry periods during the last 200,000 years documented in the clay fraction of Eastern Mediterranean deep-sea sediments.* Quaternary Science Reviews, 2021. **260**: p. 106925.
17. deMenocal, P., et al., *Abrupt onset and termination of the African Humid Period:: rapid climate responses to gradual insolation forcing.* Quaternary science reviews, 2000. **19**(1-5): p. 347-361.
18. McGee, D., et al., *The magnitude, timing and abruptness of changes in North African dust deposition over the last 20,000 yr.* Earth and Planetary Science Letters, 2013. **371**: p. 163-176.
19. Tierney, J.E. and P.B. deMenocal, *Abrupt shifts in Horn of Africa hydroclimate since the Last Glacial Maximum.* Science, 2013. **342**(6160): p. 843-846.

20. Palchan, D. and A. Torfstein, *A drop in Sahara dust fluxes records the northern limits of the African Humid Period.* Nature Communications, 2019. **10**(1): p. 3803.
21. Wassenburg, J.A., et al., *Reorganization of the North Atlantic Oscillation during early Holocene deglaciation.* Nature Geoscience, 2016. **9**(8): p. 602-605.
22. Tjallingii, R., et al., *Coherent high-and low-latitude control of the northwest African hydrological balance.* Nature Geoscience, 2008. **1**(10): p. 670-675.
23. Koren, I., et al., *The Bodélé depression: a single spot in the Sahara that provides most of the mineral dust to the Amazon forest.* Environmental Research Letters, 2006. **1**(1): p. 014005.
24. Armitage, S.J., C.S. Bristow, and N.A. Drake, *West African monsoon dynamics inferred from abrupt fluctuations of Lake Mega-Chad.* Proceedings of the National Academy of Sciences, 2015. **112**(28): p. 8543-8548.
25. Adkins, J., P. Demenocal, and G. Eshel, *The "African humid period" and the record of marine upwelling from excess 230Th in Ocean Drilling Program Hole 658C.* Paleoceanography, 2006. **21**(4).
26. Francus, P., et al., *Varved sediments of Lake Yoa (Ounianga Kebir, Chad) reveal progressive drying of the Sahara during the last 6100 years.* Sedimentology, 2013. **60**(4): p. 911-934.
27. Kröpelin, S., et al., *Climate-driven ecosystem succession in the Sahara: the past 6000 years.* science, 2008. **320**(5877): p. 765-768.
28. Gasse, F., et al., *The arid–humid transition in the Sahara and the Sahel during the last deglaciation.* Nature, 1990. **346**(6280): p. 141-146.
29. Gasse, F. and E. Van Campo, *Abrupt post-glacial climate events in West Asia and North Africa monsoon domains.* Earth and Planetary Science Letters, 1994. **126**(4): p. 435-456.
30. Drake, N.A., et al., *Ancient watercourses and biogeography of the Sahara explain the peopling of the desert.* Proceedings of the National Academy of Sciences, 2011. **108**(2): p. 458-462.
31. Cheddadi, R., et al., *Early Holocene greening of the Sahara requires Mediterranean winter rainfall.* Proceedings of the National Academy of Sciences, 2021. **118**(23): p. e2024898118.
32. Kutzbach, J., et al., *Potential role of winter rainfall in explaining increased moisture in the Mediterranean and Middle East during periods of maximum orbitally-forced insolation seasonality.* Climate Dynamics, 2014. **42**: p. 1079-1095.
33. Wagner, B., et al., *Mediterranean winter rainfall in phase with African monsoons during the past 1.36 million years.* Nature, 2019. **573**(7773): p. 256-260.
34. Hoelzmann, P., et al., *Mid-Holocene extreme precipitation in the Tibesti, Central Sahara.* Nature Communications, 2025. **16**(1): p. 7426.
35. Harrison, S.P., et al., *Evaluation of CMIP5 palaeo-simulations to improve climate projections.* Nature Climate Change, 2015. **5**(8): p. 735-743.
36. Perez-Sanz, A., et al., *Evaluation of modern and mid-Holocene seasonal precipitation of the Mediterranean and northern Africa in the CMIP5 simulations.* Climate of the Past, 2014. **10**(2): p. 551-568.
37. Pausata, F.S., G. Messori, and Q. Zhang, *Impacts of dust reduction on the northward expansion of the African monsoon during the Green Sahara period.* Earth and Planetary Science Letters, 2016. **434**: p. 298-307.
38. Lu, Z., et al., *Dynamic vegetation simulations of the mid-Holocene Green Sahara.* Geophysical Research Letters, 2018. **45**(16): p. 8294-8303.
39. Specht, N.F., M. Claussen, and T. Kleinen, *Simulated range of mid-Holocene precipitation changes from extended lakes and wetlands over North Africa.* Climate of the Past, 2022. **18**(5): p. 1035-1046.
40. Claussen, M., A. Dallmeyer, and J. Bader, *Theory and modeling of the African humid period and the green Sahara*, in *Oxford research encyclopedia of climate science*. 2017.
41. Braconnot, P., et al., *Evaluation of climate models using palaeoclimatic data.* Nature Climate Change, 2012. **2**(6): p. 417-424.

42. Braconnot, P., et al., *Results of PMIP2 coupled simulations of the Mid-Holocene and Last Glacial Maximum–Part 2: feedbacks with emphasis on the location of the ITCZ and mid-and high latitudes heat budget.* Climate of the Past, 2007. **3**(2): p. 279-296.
43. Liu, Z., et al., *Transient simulation of last deglaciation with a new mechanism for Bølling-Allerød warming.* science, 2009. **325**(5938): p. 310-314.
44. Egerer, S., et al., *The link between marine sediment records and changes in Holocene Saharan landscape: Simulating the dust cycle.* Climate of the Past, 2016. **12**(4): p. 1009-1027.
45. Gaetani, M., et al., *Understanding the mechanisms behind the northward extension of the West African Monsoon during the Mid-Holocene.* Journal of Climate, 2017. **30**(19): p. 7621-7642.
46. Hopcroft, P.O. and P.J. Valdes, *On the role of dust-climate feedbacks during the mid-Holocene.* Geophysical Research Letters, 2019. **46**(3): p. 1612-1621.
47. Cremaschi, M., et al., *Takarkori rock shelter (SW Libya): an archive of Holocene climate and environmental changes in the central Sahara.* Quaternary Science Reviews, 2014. **101**: p. 36-60.
48. Jungandreas, L., C. Hohenegger, and M. Claussen, *Influence of the representation of convection on the mid-Holocene West African Monsoon, Clim. Past, 17, 1665–1684*. 2021.
49. Jungandreas, L., C. Hohenegger, and M. Claussen, *How does the explicit treatment of convection alter the precipitation–soil hydrology interaction in the mid-Holocene African humid period?* Climate of the Past, 2023. **19**(3): p. 637-664.
50. Coulthard, T.J., et al., *Were rivers flowing across the Sahara during the last interglacial? Implications for human migration through Africa.* PloS one, 2013. **8**(9): p. e74834.
51. Larrasoaña, J.C., A.P. Roberts, and E.J. Rohling, *Dynamics of green Sahara periods and their role in hominin evolution.* PloS one, 2013. **8**(10): p. e76514.
52. Manning, K., et al., *Habitat fragmentation and the sporadic spread of pastoralism in the mid-Holocene Sahara.* Quaternary Science Reviews, 2023. **309**: p. 108070.
53. Ramírez-Pedraza, I., et al., *Arid, mosaic environments during the Plio-Pleistocene transition and early hominin dispersals in northern Africa.* Nature communications, 2024. **15**(1): p. 8393.
54. Breeze, P.S., et al., *Remote sensing and GIS techniques for reconstructing Arabian palaeohydrology and identifying archaeological sites.* Quaternary International, 2015. **382**: p. 98-119.
55. Lehner, B., K. Verdin, and A. Jarvis, *New global hydrography derived from spaceborne elevation data.* Eos, Transactions American Geophysical Union, 2008. **89**(10): p. 93-94.
56. Lehner, B. and G. Grill, *Global river hydrography and network routing: baseline data and new approaches to study the world's large river systems.* Hydrological Processes, 2013. **27**(15): p. 2171-2186.
57. Krapp, M., et al., *A statistics-based reconstruction of high-resolution global terrestrial climate for the last 800,000 years.* Scientific Data, 2021. **8**(1): p. 228.
58. Drake, N.A., et al., *Sedimentary and geomorphic evidence of Saharan megalakes: A synthesis.* Quaternary Science Reviews, 2022. **276**: p. 107318.
59. Davies, B.R. and F. Gasse, *African wetlands and shallow water bodies: Bibliography*. Vol. 1. 1988: IRD Editions.
60. Alioua, Y., et al., *Arachnid fauna of the sebkhat el melah-ramsar site in the sahara desert of Algeria.* Revista Ibérica de Aracnología, 2022. **40**(1): p. 165-169.
61. Skadhauge, E., et al., *Function of the lower intestine and osmoregulation in the ostrich: preliminary anatomical and physiological observations.* Quarterly Journal of Experimental Physiology: Translation and Integration, 1984. **69**(4): p. 809-818.
62. Grenot, C.J., *Ecophysiological characteristics of large herbivorous mammals in arid Africa and the Middle East.* Journal of Arid Environments, 1992. **23**(2): p. 125-155.

63. Weiss, L.M., *The social life of rock art: Materiality, consumption, and power in South African heritage.* Archaeologies of materiality, 2005: p. 46-70.
64. McDonald, J. and P. Veth. *The archaeology of memory: the recursive relationship of Martu rock art and place*. in *Anthropological Forum*. 2013. Taylor & Francis.
65. Porr, M. and H.R. Bell, *'Rock-art','animism'and two-way thinking: Towards a complementary epistemology in the understanding of material culture and 'rock-art'of hunting and gathering people.* Journal of Archaeological Method and Theory, 2012. **19**(1): p. 161-205.
66. Jones, A., et al., *Soil atlas of Africa*. 2013: European Union.
67. Marzin, C. and P. Braconnot, *Variations of Indian and African monsoons induced by insolation changes at 6 and 9.5 kyr BP.* Climate Dynamics, 2009. **33**(2): p. 215-231.
68. Rachmayani, R., M. Prange, and M. Schulz, *North African vegetation–precipitation feedback in early and mid-Holocene climate simulations with CCSM3-DGVM.* Climate of the Past, 2015. **11**(2): p. 175-185.
69. Kutzbach, J.E., et al., *African climate response to orbital and glacial forcing in 140,000-y simulation with implications for early modern human environments.* Proceedings of the National Academy of Sciences, 2020. **117**(5): p. 2255-2264.
70. Duque-Villegas, M., et al., *Pattern scaling of simulated vegetation change in North Africa during glacial cycles.* Climate of the Past Discussions, 2024. **2024**: p. 1-30.
71. Sereno, P.C., et al., *Lakeside cemeteries in the Sahara: 5000 years of Holocene population and environmental change.* PloS one, 2008. **3**(8): p. e2995.
72. Lézine, A.-M., et al., *Late Holocene plant and climate evolution at Lake Yoa, northern Chad: pollen data and climate simulations.* Climate of the Past, 2011. **7**(4): p. 1351-1362.
73. Castañeda, I.S., et al., *Wet phases in the Sahara/Sahel region and human migration patterns in North Africa.* Proceedings of the National Academy of Sciences, 2009. **106**(48): p. 20159-20163.
74. Thompson, L.G., et al., *Kilimanjaro ice core records: evidence of Holocene climate change in tropical Africa.* science, 2002. **298**(5593): p. 589-593.
75. Edmunds, W. and E. Wright, *Groundwater recharge and palaeoclimate in the Sirte and Kufra basins, Libya.* Journal of hydrology, 1979. **40**(3-4): p. 215-241.
76. Pachur, H.-J. and N. Altmann, *Die Ostsahara im Spätquartär: Ökosystemwandel im größten hyperariden Raum der Erde*. 2006: Springer.
77. Leggett, K.E., *Home range and seasonal movement of elephants in the Kunene Region, northwestern Namibia.* African Zoology, 2006. **41**(1): p. 17-36.
78. Liz, A.V., Rödder, D., Gonçalves, D.V., Velo-Antón, G., Paúl, M.J., Drake, N., Breeze, P., Valdes, P.V., Tarroso, P., Hopcroft, P., Crochet, P.-A., Godinho, R., Carvalho, S.B., & Brito, J.C., *The phylogeographic legacy of palaeoclimate and habitat shifts in North African vertebrates.* Nature Communications, 2026 (In press).
79. Shanahan, T.M., et al., *The time-transgressive termination of the African Humid Period.* Nature Geoscience, 2015. **8**(2): p. 140-144.
80. Haynes Jr, C., et al., *Holocene palaeoecology of the eastern Sahara; Selima Oasis.* Quaternary Science Reviews, 1989. **8**(2): p. 109-136.
81. H.-O. Pörtner, D.C.R., M. Tignor, E.S. Poloczanska, K. Mintenbeck, A. Alegría, M. Craig, S. Langsdorf, S. Löschke, V. Möller, A. Okem, B. Rama (eds.), *Climate Change 2022: Impacts, Adaptation, and Vulnerability. Contribution of Working Group II to the Sixth Assessment Report of the Intergovernmental Panel on Climate Change*. 2022, IPCC: Cambridge, UK and New York, NY, USA. p. 3056.

Supplementary Files

This is a list of supplementary files associated with this preprint. Click to download.

- SupplementaryInformation.docx